



Thermoelectric properties and electronic structure of p-type Mg₂Si and Mg₂Si_{0.6}Ge_{0.4} compounds doped with Ga

H. Ihou-Mouko^{a,*}, C. Mercier^a, J. Tobola^b, G. Pont^c, H. Scherrer^a

^a Institut Jean Lamour (I.J.L.) – UMR 7198 – Nancy-Université, Ecole Nationale des Mines de Nancy, Parc de Saurupt, F 54042 Nancy, France

^b Faculty of Physics and Applied Computer Science, AGH University of Science and Technology, Al. Mickiewicza 30, 30-059 Cracow, Poland

^c Centre National d'Etudes Spatiales (CNES), 18 avenue Edouard Belin, 31401 Toulouse Cedex 09, France

ARTICLE INFO

Article history:

Received 5 February 2011

Received in revised form 8 March 2011

Accepted 11 March 2011

Available online 21 March 2011

Keywords:

Magnesium silicide

Electronic structure

Thermoelectric properties

ABSTRACT

Mg₂Si:Ga_x and Mg₂Si_{0.6}Ge_{0.4}:Ga_x ($x = 0.4\%$ and 0.8%) solid solutions have been synthesized by direct melting in tantalum crucibles and hot pressing. The effect of Ga doping on the thermoelectric properties has also been investigated by measurements of thermopower, electrical resistivity, Hall coefficient and thermal conductivity in temperature range from 300 to 850 K. All samples exhibit a *p*-type conductivity evidenced by positive sign of both thermopower and Hall coefficient in the investigated temperatures. The maximum value of the dimensionless figure of merit ZT was reached for the Mg₂Si_{0.6}Ge_{0.4}:Ga(0.8%) compound at 625 K (ZT ~ 0.36). The *p*-type character of thermoelectric behaviours of Ga-doped Mg₂Si and Mg₂Si_{0.6}Ge_{0.4} compounds well corroborates with the results of electronic structure calculations performed by the Korringa–Kohn–Rostoker method and the coherent potential approximation (KKR-CPA), since Ga diluted in Mg₂Si and Mg₂Si_{0.6}Ge_{0.4} (on Si/Ge site) behaves as hole donor due to the Fermi level shifted to the valence band edge. The onset of large peak of DOS from Ga impurity at the valence band edge, well corroborates with high Seebeck coefficient measured in Ga-doped samples.

© 2011 Elsevier B.V. All rights reserved.

1. Introduction

Intermetallic compounds of Mg₂X (X = Si, Ge or Sn) and their solid solutions have attracted attention of many research groups as promising thermoelectric (TE) materials that can be used for heat recovery and energy conversion applications at 500–850 K temperature [1–12]. There are some reasons as environmental constraints, the abundance of constituent elements as well as the low densities (~2–3.6 g/cm³) that make these TE materials particularly appealing (ZT ~ 1), compared to PbTe or CoSb₃, used in the same temperature range. The efficiency of TE materials are commonly defined by the dimensionless figure of merit

$$ZT = \frac{\alpha^2}{\rho\kappa} T,$$

where α is thermopower, ρ the electrical resistivity, and κ the thermal conductivity at temperature T . Due to the fact that all Mg₂X compounds exhibit a semiconductor-like or semimetallic-like behaviours, most of recent investigations have been focused on solid solutions Mg₂Si_{1-x}Ge_x, Mg₂Si_{1-x}Sn_x and Mg₂Sn_{1-x}Ge_x in order to decrease electrical resistivity as well as thermal conductivity

[4–7]. It was found that bulk polycrystalline compounds showed rather high figure of merit for *n*-type materials doped with Bi (ZT ~ 0.9–1.01) [8,9] or Sb (ZT ~ 0.7–1.11) [5,10,12]. It appears that *p*-type materials are quite difficult to be stabilized in these phases. However, Noda et al. have reported the ZT value as large as 1.68 at 629 K for Ag-doped Mg₂Si_{0.6}Ge_{0.4} [5]. Conversely, latter studies [9] have rather achieved much smaller ZT values, e.g. 0.26.

In this work we present results of the chemical synthesis, X-ray diffraction characterisation and thermoelectric properties measurements in Ga-doped Mg₂Si and Mg₂Si_{0.6}Ge_{0.4} compounds. Electron transport behaviours in these systems are discussed in view of electronic band structure calculations carried out by the Korringa–Kohn–Rostoker method with the coherent potential approximation (KKR-CPA). We will show that Ga doped in Mg₂Si and Mg₂Si_{0.6}Ge_{0.4} compounds, likely diluted on Si/Ge site, yields *p*-type TE materials, characterised by relatively high ZT ~ 0.36.

2. Experimental and theoretical details

The Mg₂Si:Ga_x and Mg₂Si_{0.6}Ge_{0.4}:Ga_x powder samples ($x = 0.4\%$ and 0.8%) were prepared by alloying a stoichiometric mixture of high purity (99.999%) commercially available elements. Because of high vapour pressure of magnesium metal at elevated temperature, it was necessary to use a closed system to avoid an important loss of Mg during the thermal treatment. Hence, the starting materials were placed in Ta crucibles which were sealed by arc-welding in a glove-box under high purity argon atmosphere. The additional glassy carbon crucibles were used to recover properly and easily the alloys. The Ta container was placed into silica under secondary vacuum and annealed for 2 days at 750 °C for the first thermal treatment. The product

* Corresponding author. Tel.: +33 0383584165; fax: +33 0383584048.

E-mail address: Hilaire.Ihou-mouko@mines.inpl-nancy.fr (H. Ihou-Mouko).

of the aforementioned reaction was crushed mechanically by using an agate mortar and compacted into pellets. The pellets were again put into the glassy carbon crucible and then placed into the Ta crucibles. These Ta crucibles were put into silica under secondary vacuum and annealed for 2 days at 750 °C for the second thermal treatment.

The $\text{Mg}_2\text{Si}:\text{Ga}_x$ and $\text{Mg}_2\text{Si}_{0.6}\text{Ge}_{0.4}:\text{Ga}_x$ ($x = 0.4\%$ and 0.8%) samples were crushed and the powders were sieved below 50 μm . The powders were compacted into pellets (15 mm of diameter) using a graphite matrix by hot pressing process under 50 MPa at 800 °C during 2 h in argon atmosphere with a pressure of 50 MPa. The densities of the sintered materials were evaluated from their mass and dimensions and they represented $\sim 98\%$ of the theoretical values.

The crystalline phase and its purity for obtained samples were checked by X-ray diffraction analysis using (D8 Advance BRUKER diffractometer, $\lambda_{\text{Cu/K}\alpha} = 1.54056 \text{ \AA}$). The chemical composition of the samples was verified by electron microprobe analysis (EMPA) using a CAMECA-SX 100 device.

The thermopower (α), the electrical resistivity (ρ) and Hall coefficient (R_H) were measured as a function of temperature using light pulse technique [13] and van der Paw method [14] at in the 300–850 K temperature range. The thermal conductivity (κ) was derived from the equation $\kappa = a \cdot C_p \cdot d$ that includes the experimental thermal diffusivity (a), the heat capacity (C_p) and the material density (d). The thermal diffusivity and the heat capacity were measured (300–850 K) using a laser flash technique (NETZSCH LFA 427) and a differential scanning calorimeter (DSC), respectively.

Electronic structure computations were performed using the Korringa–Kohn–Rostoker (KKR) method in ordered parent compounds Mg_2Si and Mg_2Ge . To account for chemical disorder in $\text{Mg}_2\text{Si}_{1-x}\text{Ge}_x$ alloys, the coherent potential approximation (CPA) has been incorporated into the KKR technique [15,16]. The crystal potential of muffin-tin form was constructed within the local density approximation (LDA) framework, using von Barth–Hedin parameterization for the exchange–correlation potential. For well-converged charges and potentials (below 0.1 mRy), the total, site-decomposed, and l -decomposed density of states (DOS) were computed applying k -space tetrahedron integration. The Fermi level was precisely determined from the generalized Lloyd formula [17]. The electronic band structure with complex energy was also computed in selected alloys along high-symmetry directions in the Brillouin zone.

The influence of Ga dopant on the DOS and dispersion curves $E(\mathbf{k})$ in the host material was examined in more detail in the case of Mg_2Si and $\text{Mg}_2\text{Si}_{0.6}\text{Ge}_{0.4}$, corresponding to the experimentally investigated samples. Since a small amount of introduced Ga is actually hardly detectable by standard EPMA analysis, the KKR-CPA runs have been done considering dilution on two nonequivalent crystallographic sites. This selective substitution with Ga has allowed to establish n or p character of carriers, basing on DOS analysis in the vicinity of the Fermi level. Note, that when diluting Ga in $\text{Mg}_2\text{Si}_{0.6}\text{Ge}_{0.4}$, the “disordered” site contained three atoms randomly distributed on the same crystallographic position. This case required to extend the self-consistent CPA condition for Green function G_{CP} , to more general form $G_{\text{CP}} = \sum_i c_i G_i$ with $\sum_i c_i = 1$.

Furthermore, preliminary information on thermopower behaviour in investigated series of compounds, has been estimated from the Mott’s formula:

$$\frac{\alpha}{T} = -\frac{\pi^2 k_B^2}{3e} \frac{\partial \ln \sigma(E)}{\partial E}$$

at $E = E_F$. Assuming that the transport function $\sigma(E)$ is mainly driven by DOS at the Fermi level and the hole mobility is energy independent, the transport function (containing complete information on k -dependent velocities and relaxation times of electrons) can be replaced by total DOS, $n(E)$. Consequently, the linear part of thermopower can be derived, accounting only for $n(E)$ and its derivative $dn(E)/dE$ at the Fermi level, yielding

$$\frac{\alpha}{T} \approx -\frac{1}{n(E)} \frac{dn(E)}{dE}$$

at $E = E_F$. This approach allowed tentatively interpreting positive sign and large values of thermopower observed in Ga-doped $\text{Mg}_2(\text{Si}-\text{Ge})$ systems.

In all calculations of ordered and disordered systems, the experimental values of lattice constants were employed.

3. Experimental and theoretical results

3.1. Crystal-chemistry and sample purity

The X-ray diffraction patterns indicate that the all compounds studied crystallize in the cubic anti-fluorite CaF_2 -type structure ($Fm-3m$ space group). The lattice parameters were determined by Rietveld profile refinements using the software Fullprof [18] (see Table 1). The replacement of Si atoms by the larger Ge atoms leads to a small increase ($\sim 0.2\%$) of the lattice parameter, which remains in agreement with previous data [4,7]. We have also observed that the

Table 1

Lattice parameter (a) and densities (d and d_t) of Ga-doped Mg_2Si and $\text{Mg}_2\text{Si}_{0.6}\text{Ge}_{0.4}$ compounds. Relative density (dr) denotes the ratio of measured and theoretical density.

Chemical composition	a (Å)	d (g/cm ³)	dr (%)
$\text{Mg}_2\text{Si}:\text{Ga}(0.4\%)$	6.354 (3)	1.98	0.99
$\text{Mg}_2\text{Si}:\text{Ga}(0.8\%)$	6.355 (3)	1.96	0.98
$\text{Mg}_2\text{Si}_{0.6}\text{Ge}_{0.4}:\text{Ga}(0.4\%)$	6.368 (3)	2.43	0.98
$\text{Mg}_2\text{Si}_{0.6}\text{Ge}_{0.4}:\text{Ga}(0.8\%)$	6.369 (3)	2.42	0.98

Ga doping very slightly increases the unit volume when compared to undoped compounds.

Electron microprobe analysis measurements have evidenced no significant deviation from the ideal 2:1 atomic ratio between Mg and Si/Ge. However, after hot pressing process experimental concentrations of Ga have been found to be lower than the nominal concentrations (0.4% and 0.8% instead of 1% and 2%, respectively), indicating serious difficulty to enter more Ga into the matrix. Both microanalysis and X-ray diffraction have also revealed the presence of small amount of silicon (less than 2–5 wt.%).

3.2. Thermoelectric properties

The thermal variation (300–850 K) of the electrical resistivity of Ga-doped Mg_2Si and $\text{Mg}_2\text{Si}_{0.6}\text{Ge}_{0.4}$ compounds is shown in Fig. 1. All ρ (T) curves decrease with increasing temperature, indicating a semiconductor-like behaviour, and they tend to more or less similar values at high temperature. The room-temperature ρ of Ga-doped Mg_2Si compounds are visibly larger than those of Ga-doped $\text{Mg}_2\text{Si}_{0.6}\text{Ge}_{0.4}$ ones. Moreover, with increasing Ga content, both electrical resistivity and its slope decrease, that would suggest a crossover to from semiconducting-like to semimetallic-like behaviour. This is best seen for $\text{Mg}_2\text{Si}_{0.6}\text{Ge}_{0.4}:\text{Ga}(0.8\%)$, where the electrical resistivity only slowly decreases in the whole temperature range. Interestingly, the Si/Ge alloying and p -type doping affected the electrical resistivity curves in quite similar way as in Ag-doped Mg_2Si and $\text{Mg}_2\text{Si}_{0.6}\text{Ge}_{0.4}$ compounds [9], but the electrical resistivity was found to decrease more rapidly in the latter.

The results of the Hall coefficient R_H , carrier mobility μ_H and carrier concentration n_p at room temperature (RT) are presented in Table 2. The R_H values are positive for all compounds, indicating a p -type conductivity mechanism related to holes. The RT carrier mobility μ_H and carrier concentration n_p increase with increasing Ga content, both for $\text{Mg}_2\text{Si}:\text{Ga}_x$ and $\text{Mg}_2\text{Si}_{0.6}\text{Ge}_{0.4}:\text{Ga}_x$ compounds. Ga-doped Mg_2Si compounds exhibit the n_p and μ_H values significantly lower than those of Ga-doped $\text{Mg}_2\text{Si}_{0.6}\text{Ge}_{0.4}$ compounds,

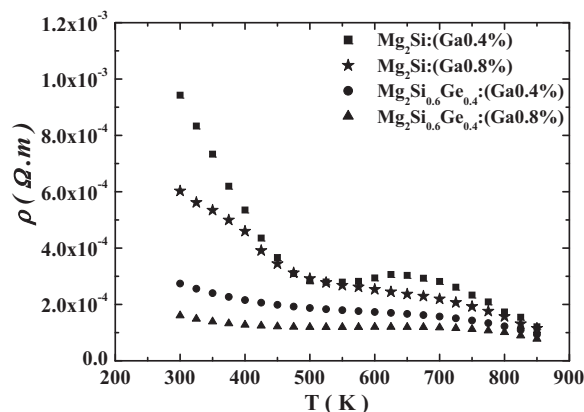
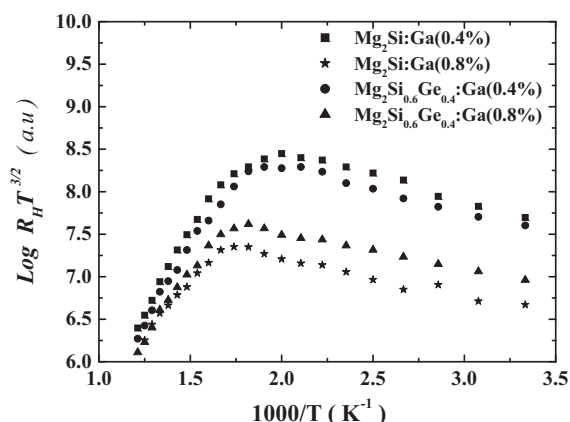


Fig. 1. Electrical resistivity (ρ) of $\text{Mg}_2\text{Si}:\text{Ga}_x$ and $\text{Mg}_2\text{Si}_{0.6}\text{Ge}_{0.4}:\text{Ga}_x$ ($x = 0.4\%$ and 0.8%) compounds.

Table 2Experimental values of electron transport properties of Ga-doped Mg₂Si and Mg₂Si_{0.6}Ge_{0.4} compounds at RT.

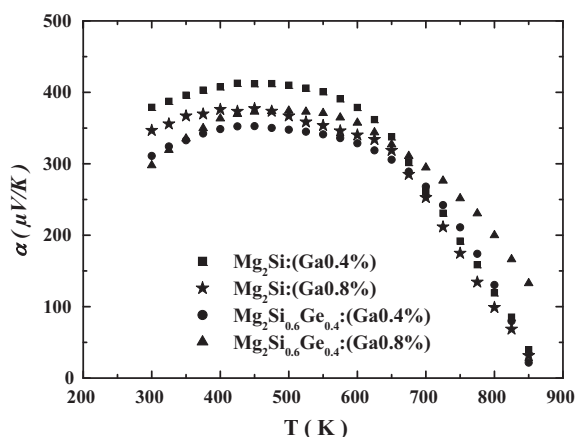
Chemical composition	ρ (Ω m)	R_H ($\text{cm}^3 \text{C}^{-1}$)	n_p (cm^{-3})	μ_H ($\text{cm}^2 \text{V}^{-1} \text{s}^{-1}$)	α (μVK^{-1})	n_F	m_p^*/m_0	E_g (eV)
Mg ₂ Si:Ga(0.4%)	9.43×10^{-4}	0.460	1.36×10^{19}	4.87	380	0.75	1.08	0.79
Mg ₂ Si:Ga(0.8%)	6.03×10^{-4}	0.386	1.62×10^{19}	6.39	347	0.82	1.11	0.75
Mg ₂ Si _{0.6} Ge _{0.4} :Ga(0.4%)	2.74×10^{-4}	0.203	3.08×10^{19}	7.36	310	0.91	1.52	0.73
Mg ₂ Si _{0.6} Ge _{0.4} :Ga(0.8%)	1.60×10^{-4}	0.198	3.29×10^{19}	11.84	300	0.94	1.54	0.68

**Fig. 2.** $\text{Log}(R_H T^{3/2}) = f(1/T)$ of Mg₂Si:Ga_x and Mg₂Si_{0.6}Ge_{0.4}:Ga_x ($x = 0.4\%$ and 0.8%) compounds.

which remains in line with the aforementioned behaviours of the electrical resistivity curves showing more semimetallic character of the latter.

In intrinsic region, the energy gap at absolute zero E_g , may be estimated from the slope of a plot of $\text{Log}(R_H T^{3/2}) = f(1/T)$ (see, Fig. 2). The energy gap, as obtained by least-squares fits to the data in the linear region is given in Table 2. These values of energy gap E_g are between 0.79 eV for Mg₂Si:Ga(0.4%) and 0.68 eV for Mg₂Si_{0.6}Ge_{0.4}:Ga(0.8%), values very close to those reported by several authors for the Mg₂Si_{1-x}Ge_x solid solution [1,2,4,5,19].

Fig. 3 shows the temperature dependences of the thermopower of Ga-doped Mg₂Si and Mg₂Si_{0.6}Ge_{0.4} compounds. The sign of the Seebeck coefficient of all compositions is positive, which well corroborates *p*-type conductivity observed from Hall coefficient R_H measurements. All $\alpha(T)$ curves present a maximum, being the most pronounced for the case of Mg₂Si:Ga(0.4%). The thermopower maximum slightly shifts towards higher tem-

**Fig. 3.** Thermopower (α) of Mg₂Si:Ga_x and Mg₂Si_{0.6}Ge_{0.4}:Ga_x ($x = 0.4\%$ and 0.8%) compounds.

peratures with increasing Ga content both for Mg₂Si:Ga and Mg₂Si_{0.6}Ge_{0.4}:Ga compounds. Within the investigated samples, the largest thermopower value is $\sim 412 \mu\text{V/K}$ (at 475 K) obtained for Mg₂Si:Ga(0.4%).

It is possible to obtain some information about the effective masses of holes m_p^* at RT from experimental results of the thermopower α , and carrier concentration n_p . These effective masses m_p^* were calculated within a single parabolic band model and assuming that the acoustic phonon scattering is the predominant mechanism at RT for Ga-doped Mg₂Si and Mg₂Si_{0.6}Ge_{0.4} alloys, as reported by LaBotz et al. [4] and Noda et al. [5]. The thermopower α and carrier concentration n_p are given by:

$$\alpha = \frac{k_B}{e} \left(\frac{2F_1(n_F)}{F_0(n_F)} - n_F \right)$$

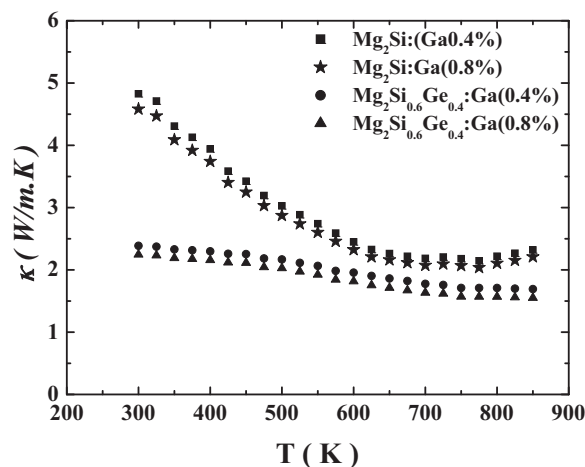
$$n_p = 4\pi \left(2m_p^* \times \frac{k_B T}{h^2} \right)^{3/2} F_{1/2}(n_F)$$

with

$$F_i(n_F) = \int_0^\infty \frac{x^i dx}{1 + e^{(x-n_F)}}$$

where $F_i(n_F)$ are the Fermi-Dirac integrals, n_F the reduced Fermi level, k_B the Boltzmann constant and h the Planck constant. The values of reduced effective masses of holes m_p^*/m_0 , where m_0 is the mass of the free electron obtained at RT are given in Table 2. As can be seen, these values increase with increasing carrier concentration n_p and Ga content, suggesting that the band structure is modified by the Ga doping (in particular the hole bands near E_F , which are responsible for transport of charge carriers).

The thermal conductivity of Ga-doped Mg₂Si and Mg₂Si_{0.6}Ge_{0.4} compounds is shown in Fig. 4. In both cases, the thermal conductivity (κ) decreases with increasing Ga content. The κ values of Ga-doped Mg₂Si compounds reaches a minimum (at ~ 700 K) 2.3 and 2.4 W/mK for Mg₂Si:Ga(0.4%) and Mg₂Si:Ga(0.8%), respec-

**Fig. 4.** Thermal conductivity (κ) of Mg₂Si:Ga_x and Mg₂Si_{0.6}Ge_{0.4}:Ga_x ($x = 0.4\%$ and 0.8%) compounds.

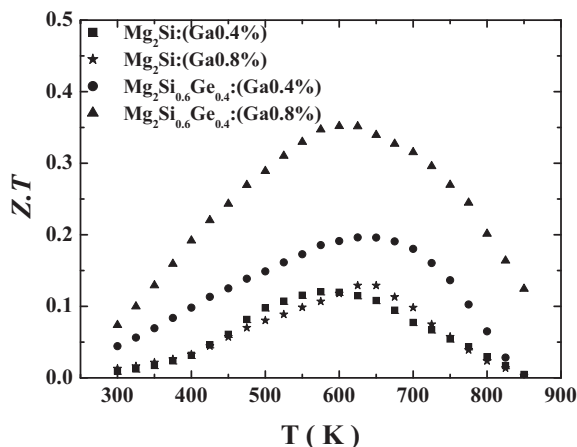


Fig. 5. Temperature dependence ZT of $\text{Mg}_2\text{Si}:\text{Ga}_x$ and $\text{Mg}_2\text{Si}_{0.6}\text{Ge}_{0.4}:\text{Ga}_x$ ($x=0.4\%$ and 0.8%) compounds.

tively. Conversely, the Ga-doped $\text{Mg}_2\text{Si}_{0.6}\text{Ge}_{0.4}$ compounds exhibit thermal conductivities that slowly decrease with increasing temperature and these values are lower compared to those found in Ga-doped Mg_2Si compounds. This decrease of thermal conductivity of Ga-doped $\text{Mg}_2\text{Si}_{0.6}\text{Ge}_{0.4}$ compounds can be likely attributed to Si/Ge disorder in the $\text{Mg}_2\text{Si}_{1-x}\text{Ge}_x$ alloys, as reported by Akasaka et al. [7].

Accounting for the thermal conductivity κ of a material is commonly expressed by a sum of a electronic (κ_{el}) and lattice (κ_{ph}) contributions ($\kappa = \kappa_{el} + \kappa_{ph}$), the first part can be calculated from the Wiedemann–Franz law $\kappa_{el} = L_0 T / \rho$ (L_0 : Lorentz number $2.45 \times 10^{-8} \text{ V}^2/\text{K}^2$, ρ : electrical resistivity, T : absolute temperature). The lattice contribution (κ_{ph}) is simply obtained from a difference between total and electronic thermal conductivities $\kappa_{ph} = \kappa - \kappa_{el}$.

In our samples, the electronic thermal conductivity (κ_{el}) is much lower than the lattice part and is of order of 0.15 W/mK being almost independent of temperature. The values of lattice thermal conductivities κ_{ph} obtained in our investigated samples shows that for all compounds, this phonon thermal conductivity (κ_{ph}) dominates the magnitude as well as the temperature dependence of total thermal conductivity (κ), indicating that phonon-phonon interactions are predominantly responsible for the character of thermal resistance.

We can note that the values of thermal conductivities measured for Ga-doped Mg_2Si and $\text{Mg}_2\text{Si}_{0.6}\text{Ge}_{0.4}$ are comparable to the κ values reported for undoped samples [4,7], also varying between 6.9 and 3.2 W/mK for Mg_2Si and 2.5 – 2.1 W/mK for $\text{Mg}_2\text{Si}_{0.6}\text{Ge}_{0.4}$.

The dimensionless figure of merit ZT was calculated from the measured electrical resistivity (ρ), thermopower (α) and thermal conductivity (κ) as a function of temperature.

Fig. 5 shows the thermal variation curves of ZT for p-type $\text{Mg}_2\text{Si}:\text{Ga}_x$ and $\text{Mg}_2\text{Si}_{0.6}\text{Ge}_{0.4}:\text{Ga}_x$ ($x=0.4\%$ and 0.8%) compounds. For the all compounds, the ZT values increase with the temperature increasing then decrease after reaching maximum values between ~ 600 and 650 K . The maximum ZT value of ~ 0.36 is obtained at 625 K for $\text{Mg}_2\text{Si}_{0.6}\text{Ge}_{0.4}:\text{Ga}(0.8\%)$.

3.3. Theoretical results

The Mg_2Si compound exhibits an indirect Γ –X energy gap (E_g) of order of 0.2 – 0.3 eV from our KKR method, being in line with very recent electronic calculations [20]. Much larger experimental values of E_g , ranging from 0.66 to 0.78 eV [1,21,22], have been well interpreted from the GW method [23], yielding $E_g = 0.65 \text{ eV}$.

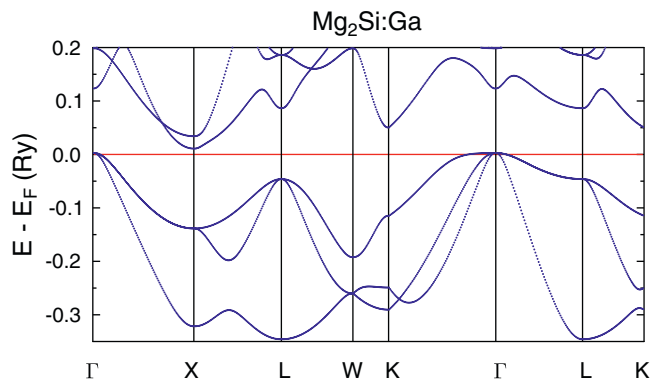


Fig. 6. The real part of electronic dispersion curves of Ga-doped Mg_2Si compound (Ga on Si-site).

Electronic structure calculations commonly revealed that the band gap comes from strong hybridization of p -states of Mg and (s,p)-states of Si. From the chemical point of view, the crystal structure of Mg_2X ($X = \text{Si}, \text{Ge}, \text{Sn}$) is stabilized by covalent sp^3 bonding for particular number of peripheral electrons (VEC). For divalent Mg and tetravalent X elements, the bonds are completely filled for $\text{VEC} = 8$ ($2 \times 2 + 4$), which is manifested by formation of energy gap above fourth valence band [9,11,20]. The top of valence bands is triply degenerated at Γ point (Fig. 6), which is generally favourable to increase thermopower. Noteworthy, one of the valence bands (well seen along Γ –K direction) is much more flat than the others, which suggests relatively heavy effective hole masses, being favourable for thermopower enhancement. Unlikely, at the bottom of the conduction bands (X point) there are two intersecting bands, which are non-degenerated [6,9,11]. It is interesting to remind that the degeneracy of these two conduction bands may appear when Si is substituted with Sn [6], which is likely related to the expansion of the unit cell. Contrary, this unusual electronic structure feature does not occur when alloying with Ge, likely due to smaller variation of the lattice constant in $\text{Mg}_2\text{Si}_{1-x}\text{Ge}_x$ alloy [9].

Bearing in mind that LDA generally tends to underestimate measured value of energy gap, we focus mostly on the shape of valence and conduction electronic bands, as well as the effect of impurity energy levels on overall DOS in the vicinity of the Fermi level. It should be noted that our previous electronic structure computations showed that alloying isoelectronic Mg_2Si and Mg_2Ge compounds does not lead to substantial modifications of electronic bands near the energy gap [9]. This is mostly due to very close crystal potentials of Si and Ge, which is reflected as similar shape of their corresponding component DOSs (Fig. 3b in [9]).

In the case of Ga-doped samples, it can be noticed that Ga introduced to Mg_2Si (also to $\text{Mg}_2\text{Si}_{0.6}\text{Ge}_{0.4}$) may behave either as an electron or hole donor, depending on the crystallographic site, it is diluted. Ga substituting Mg, delivers electrons to the system and the Fermi level is placed on increasing conduction-like DOS, which suggests negative thermopower. This result would contradict with positive thermopower measured experimentally in our Ga-doped samples. Conversely, Ga substituting Si in Mg_2Si (Fig. 7) forms important p -DOS peak at the valence band edge and the Fermi level lies on strongly decreasing DOS slope. This prediction well supports positive thermopower detected in real samples $\text{Mg}_2\text{Si}:\text{Ga}_x$ and $\text{Mg}_2\text{Si}_{0.6}\text{Ge}_{0.4}:\text{Ga}_x$.

The fact that Ga impurity constitutes sharp peak in the vicinity of E_F (Fig. 7) indicates that valence states are strongly modified and both density of states $n(E_F)$ its derivative $dn(E_F)/dE$ visibly depend on Ga contents. This result suggests that a simple rigid band model, often used when predicting electron transport behaviours in doped

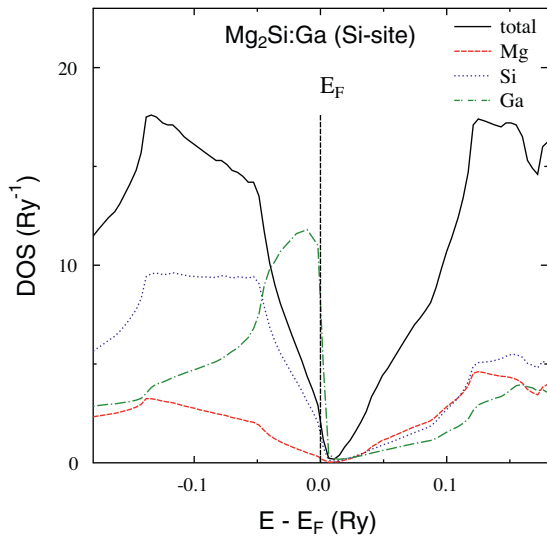


Fig. 7. Total and site-decomposed DOSs of Ga-doped $\text{Mg}_2\text{Si}:\text{Ga}_x$ ($x=0.01$) compound (Ga diluted on Si site).

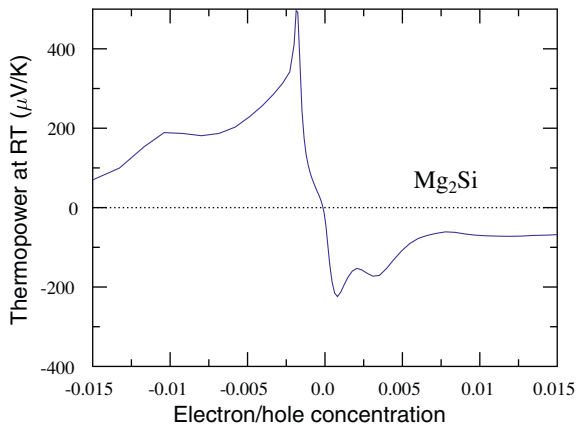


Fig. 8. RT thermopower as a function of electron or hole concentration deduced from KKR-CPA DOS in Mg_2Si .

systems, in principle fails in the case of Ga doping. On the other hand, for impurities having close crystal potential to the atom that they substitute (e.g. Bi [9] or Sb [11] replacing Si in Mg_2Si), this approach seems to be well justified.

Fig. 6 presents the real part of complex energy bands in disordered $\text{Mg}_2\text{Si}:\text{Ga}$ alloy. One observes that at 0.8% Ga concentration, E_F shifts to the valence bands edge and it cuts three hole-like pockets centered at Γ point. It appears that the highest valence band becomes even more flat when the Ga concentration increases. Inspecting in more details DOS in Ga-doped near the energy band edge and applying the simplified Mott's formula for thermopower slope α/T , one can conclude that quite large values of thermopower can be expected both in Mg_2Si (Fig. 8) and $\text{Mg}_2\text{Si}_{0.6}\text{Ge}_{0.4}$ containing the amount of Ga smaller than 1%. Depending on Ga content (actu-

Table 3
Seebeck coefficient derived from KKR-CPA DOS and Mott's formula in Ga-doped Mg_2Si and $\text{Mg}_2\text{Si}_{0.6}\text{Ge}_{0.4}$ compounds at RT, compared to experimental values.

Chemical composition	$n(E_F)$ (Ry^{-1} per f.u)	α (th) (μVK^{-1})	α (exp) (μVK^{-1})
$\text{Mg}_2\text{Si}:\text{Ga}(0.4\%)$	2.2	310	380
$\text{Mg}_2\text{Si}:\text{Ga}(0.8\%)$	2.7	195	347
$\text{Mg}_2\text{Si}_{0.6}\text{Ge}_{0.4}:\text{Ga}(0.4\%)$	2.3	275	310
$\text{Mg}_2\text{Si}_{0.6}\text{Ge}_{0.4}:\text{Ga}(0.8\%)$	2.6	192	300

ally varying hole concentration) thermopower may reach even 300–400 $\mu\text{V}/\text{K}$ at room temperature. Table 3 presents the Seebeck coefficient values computed from the KKR-CPA density of states and Mott's formula for $\text{Mg}_2\text{Si}:\text{Ga}_x$ and $\text{Mg}_2\text{Si}_{0.6}\text{Ge}_{0.4}:\text{Ga}_x$ (at RT) which well supports the experimental findings at $x=0.4\%$. The discrepancy between theoretical and experimental values of thermopower is much more important for $x=0.8\%$, which may suggest that the real amount of Ga in the alloys is smaller. On the other hand, we should bear in mind that this estimation of thermopower should be taken with care, since it is based on DOS analysis, without accounting for transport parameters as relaxation time and velocities [24] and such simplified analysis tends to underestimate the measured Seebeck coefficient.

4. Summary and conclusions

We have presented experimental and theoretical investigations on the effect of Ga doping in Mg_2Si and $\text{Mg}_2\text{Si}_{0.6}\text{Ge}_{0.4}$ compounds by measurements electrical resistivity, thermopower, Hall coefficient and thermal conductivity as well as electronic band-structure calculations. Such minute amount of impurities are sufficient to modify the thermoelectric properties of the aforementioned Mg_2Si and $\text{Mg}_2\text{Si}_{0.6}\text{Ge}_{0.4}$ compounds. All samples are p-type materials evidenced by positive sign of both thermopower and Hall coefficient in the investigated temperatures. The temperature dependence of electrical resistivity ρ decreases with Ga content and revealed that all materials are heavily doped semiconductors with the energy gaps E_g , ranging between 0.68 eV and 0.79 eV. The increase of effective mass of holes with Ga content as well as carrier concentration suggest that the band structures is modified by Ga doping. The p-type character of thermoelectric behaviours of Ga-doped Mg_2Si and $\text{Mg}_2\text{Si}_{0.6}\text{Ge}_{0.4}$ compounds, as well as the modification of bands structures are well supported by our theoretical discussion from the KKR-CPA calculations. One observes overall qualitative agreement between experimental and theoretical values of thermopower at RT, but the simplified analysis based only on calculated DOSs and Mott's formula to reach the slope α/T , tends to underestimate the measured Seebeck coefficient. The thermal conductivity κ of Ga-doped Mg_2Si and $\text{Mg}_2\text{Si}_{0.6}\text{Ge}_{0.4}$ compounds decreases with the increase Ga content. The maximum ZT value of ~ 0.36 is obtained at 625 K for $\text{Mg}_2\text{Si}_{0.6}\text{Ge}_{0.4}:\text{Ga}(0.8\%)$. This study shows that the Ga doping give the possibility to obtain p-type thermoelectric materials in $\text{Mg}_2\text{Si}_{1-x}\text{Ge}_x$ alloys.

Acknowledgements

This work was supported by the CNES (Centre National d'Etude Spatiale, Toulouse-France) on the project "Nouveaux Elements Peltier" and the FP7-NMP-2010-SMALL-4 Collaborative Project "ThermoMag" (No. 263207).

References

- [1] R.G. Morris, R.D. Redin, G.C. Danielson, Phys. Rev. 109 (1958) 1909.
- [2] R.D. Redin, R.G. Morris, G.C. Danielson, Phys. Rev. 109 (1958) 1916.
- [3] M.W. Heller, G.C. Danielson, J. Phys. Chem. Solids 23 (1962) 601.
- [4] R.J. Labotz, D.R. Mason, D.F. O'Kane, J. Electrochem. Soc. 110 (1963) 127.
- [5] Y. Noda, H. Kon, Y. Furukawa, I.A. Nishida, K. Masumoto, Mater. Trans. JIM 33 (1992) 851.
- [6] V.K. Zaitsev, M.I. Fedorov, E.A. Gurieva, I.S. Eremin, P.P. Konstantinov, A. Yu. M.V. Vedernikov, Phys. Rev. B 74 (2006) 045207.
- [7] M. Akasaka, T. Iida, K. Nishio, Y. Takahashi, Thin Solid Films 515 (2007) 8237.
- [8] J.I. Tani, H. Kido, Physica B 364 (2005) 218.
- [9] K. Mars, H. Ihou-Mouko, G. Pont, J. Tobola, H. Scherrer, J. Electron. Mater. 38 (2009) 1360.
- [10] J.I. Tani, H. Kido, Intermetallics 15 (2007) 1202.
- [11] J. Tobola, S. Kaprzyk, H. Scherrer, J. Electron. Mater. 39 (2010) 2064.
- [12] W. Liu, X. Tang, J. Sharp, J. Phys. D: Appl. Phys. 43 (2010) 085406.
- [13] L.J. Van der Pauw, Philips Res. Rep. 13 (1958) 1.

- [14] C. Wood, L.D. Zoltan, G. Stapfer, *Rev. Sci. Instrum.* 56 (1985) 719.
- [15] A. Bansil, S. Kaprzyk, P.E. Mijnarends, J. Tobola, *Phys. Rev. B* 60 (1999) 13396.
- [16] T. Stopa, S. Kaprzyk, J. Tobola, *J. Phys. Condens. Matter* 16 (2004) 4921.
- [17] S. Kaprzyk, A. Bansil, *Phys. Rev. B* 42 (1990) 7358.
- [18] J. Rodriguez-Carvajal, *Physica B* 192 (1993) 55.
- [19] E. Ratai, M.P. Augustine, S.M. Kauzlarich, *J. Phys. Chem. B* 107 (2003) 12573.
- [20] P. Boulet, M.J. Verstraete, J.-P. Crocombette, M. Briki, M.-C. Record, *Comp. Mater. Sci.* 50 (2010) 847.
- [21] P. Koenig, D. Lynch, G. Danielson, *J. Phys. Chem. Sol.* 20 (1961) 122.
- [22] F. Vazquez, R.A. Forman, M. Cardona, *Phys. Rev.* 176 (1968) 905.
- [23] B. Arnaud, M. Alouani, *Phys. Rev. B* 64 (2001) 033202.
- [24] T. Stopa, J. Tobola, S. Kaprzyk, E.K. Hlil, D. Fruchart, *J. Phys.: Condens. Matter* 18 (2006) 6379.